Progress In Electromagnetics Research B, Vol. 5, 63–76, 2008

A SYMMETRICAL CIRCUIT MODEL DESCRIBING ALL KINDS OF CIRCUIT METAMATERIALS

T. J. Cui, H. F. Ma, R. Liu, B. Zhao, Q. Cheng and J. Y. Chin

State Key Laboratory of Millimeter Waves
Department of Radio Engineering, Southeast University
Nanjing 210096, China

Abstract—We present a generally symmetrical circuit model to describe all kinds of metamaterials with effective permittivity and permeability. The model is composed of periodic structures whose unit cell is a general T-type circuit. Using the effective medium theory, we derive analytical formulations for the effective permittivity and effective permeability of the circuit model, which are quite different from the published formulas [1, 2]. Rigorous study shows that such a generally symmetrical model can represent right-handed materials, left-handed materials, pure electric plasmas, pure magnetic plasmas, electric-type and magnetic-type crystal bandgap materials at different frequency regimes, with corresponding effective medium parameters. Circuit simulations of real periodic structures and theoretical results of effective medium models in this paper and in [1] and [2] are presented. The comparison of such results shows that the proposed medium model is much more accurate than the published medium model [1, 2] in the whole frequency band.

1. INTRODUCTION

Recently, metamaterials have become hot topics in physics and electromagnetic engineering [1–23]. The implementation of metamaterials using circuit models has been well investigated in the past few years [1–12]. The well-known representations include the composite right/left-handed (CRLH) periodic structures and the LC-loaded transmission-line (TL) structures. Using the CRLH model, right-handed (RH) materials, left-handed (LH) materials, pure electric plasmas, and pure magnetic plasmas can be represented in different frequency regimes [1, 5]. Using the LC-loaded TL structures, the RH and LH materials

can be described depending on the positions of the loaded inductor (L) and capacitor (C) [2, 7]. Recently, a general LC-loaded TL structure has been proposed [12], which can also describe the RH materials, LH materials, pure electric and pure magnetic plasmas in different frequency bands.

In this paper, we present a general symmetrical circuit model to describe all kinds metamaterials, including the crystal bandgap materials [13, 14]. The model is composed of periodic structures whose unit cell is a general T-type circuit made of series and shunt capacitors and inductors. We derive analytical formulations for the effective permittivity and permeability from the effective medium theory, which are quite different from the published formulas [1, 2]. For any given values of inductances and capacitances, we obtain four critical frequencies. Such four frequencies divide the whole frequency band into five regions, which correspond to the crystal bandgap mode (electric or magnetic type), the propagating mode (right-handed or left-handed type), and pure plasma mode (electric or magnetic type). Hence the proposed general circuit model can describe right-handed (RH) materials, LH materials, pure electric plasmas, pure magnetic plasmas, electric-type crystal bandgap materials, and magnetic-type crystal bandgap materials at different frequency regimes. In order to compare the validity and accuracy of the proposed medium model with the published medium model [1, 2] in representing the periodic circuit structures, we make circuit simulations of real periodic structures and theoretical calculations of effective medium models. The simulation and analytical results show that the proposed medium model is much more accurate than the published medium model [1, 2] in the whole frequency band.

2. SYMMETRICAL CIRCUIT MODEL AND EFFECTIVE MEDIUM THEORY

We consider a general two-port network as shown in Fig. 1(a), which is an infinite periodic structure with series impedance Z_s and shunt admittance Y_p. The period of the structure is p, *which can be arbitrarily large*. This is quite different from the conventional requirements in CRLH and LC-loaded TL structures [1, 2]. We choose the unit cell of the periodic structure in a symmetrical T form [6], which includes two series impedance $Z_s/2$ and a shunt admittance Y_p, as demonstrated in Fig. 1(b).

In a general case, the impedance Z_s is composed of a series inductor L_s and a series capacitor C_s, and the admittance Y_p is composed of a shunt inductor L_p and a shunt capacitor C_p. Hence

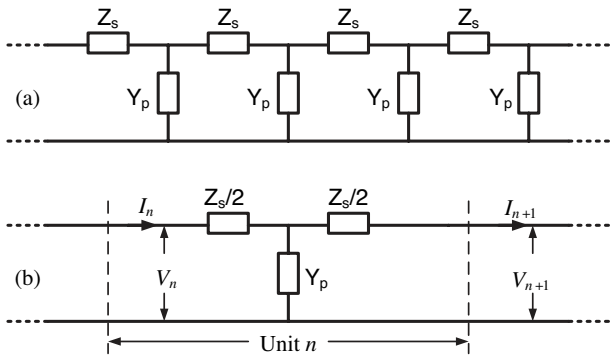

Figure 1. (a) A general periodic structure of series impedance and shunt admittance. (b) The T-type unit cell of the periodic structure.

we easily obtain $Z_s = -i\omega L_s - 1/(i\omega C_s)$ and $Y_p = -i\omega C_p - 1/(i\omega L_p)$. Based on the Bloch theorem, we have

$$I_{n+1} = I_n e^{i\theta}, \quad V_{n+1} = V_n e^{i\theta}, \tag{1}$$

where $\theta = kp$ is the phase advance across one unit cell, and k is the wavenumber. From the circuit theory, we obtain

$$V_n = V_{n+1} + I_n Z_s/2 + I_{n+1} Z_s/2, \tag{2}$$
$$I_n = I_{n+1} + (V_n - I_n Z_s/2) Y_p. \tag{3}$$

From Eqs. (1)–(3), we easily derive the dispersion equation as

$$\sin^2(\theta/2) = ZY/4, \tag{4}$$

and the wave impedance as

$$Z_0 = V_n/I_n = \frac{1}{2} Z/\tan(\theta/2), \tag{5}$$

in which

$$Z = \omega L_s - 1/(\omega C_s), \quad Y = \omega C_p - 1/(\omega L_p) \tag{6}$$

are real numbers, either positive or negative.

Depending on different values of Z and Y, the dispersion equation describes three kinds of modes [15], which are discussed in details below.

Case 1: $0 \leq ZY \leq 4$. In such a case, θ is a real number based on the dispersion equation, which corresponds to propagating modes:

$$\theta = \pm 2 \arcsin(\sqrt{ZY}/2). \tag{7}$$

When Z and Y are both positive, θ is positive, which represents a forward propagating mode; when Z and Y are both negative, θ is negative, which represents a backward propagating mode.

Case 2: $ZY < 0$. In such a case, θ is a pure imaginary number based on Eq. (4), which corresponds to pure plasma modes:

$$\theta = \pm i 2 \text{arcsinh}(\sqrt{-ZY}/2). \tag{8}$$

When "$-$" is taken, it represents an active case; when "$+$" is taken, it represents a passive case. For the considered unit cell, it is apparently the passive case.

Case 3: $ZY > 4$. In such a case, θ will be a complex number: $\theta = \theta_R + i\theta_I$, which corresponds to resonant crystal bandgap modes:

$$\theta = \pm \pi + i 2 \text{arccosh}(\sqrt{ZY}/2). \tag{9}$$

For similar reasons, only the passive case is considered in the above equation.

Based on above discussions, $ZY = 0$ and $ZY = 4$ will define boundaries of such three kinds of modes. From $ZY = 0$ and Eq. (6), we obtain two critical frequencies

$$\omega_1 = \min\{\omega_s,\ \omega_p\}, \quad \omega_2 = \max\{\omega_s,\ \omega_p\}, \tag{10}$$

in which $\omega_s = 1/\sqrt{L_s C_s}$ and $\omega_p = 1/\sqrt{L_p C_p}$ are resonant frequencies of the series and shunt branches, respectively.

Similarly, $ZY = 4$ and Eq. (6) define the other two critical frequencies:

$$\omega_3 = \sqrt{\omega_c^2 - \omega_d^2}, \quad \omega_4 = \sqrt{\omega_c^2 + \omega_d^2}, \tag{11}$$

in which $\omega_c^2 = 2/(L_s C_p) + (\omega_s^2 + \omega_p^2)/2$ and $\omega_d^4 = \omega_c^4 - \omega_s^2 \omega_p^2$. The four critical frequencies satisfy the following relation

$$\omega_3 < \omega_1 < \omega_2 < \omega_4. \tag{12}$$

Hence the whole frequency regime is divided into five regions by the four critical frequencies, as shown in Fig. 2.

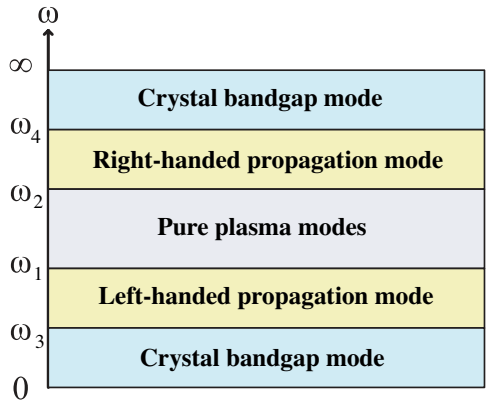

Figure 2. Different wave modes of the general periodic structure.

In regions $\omega_3 < \omega < \omega_1$ and $\omega_2 < \omega < \omega_4$, we have $0 < ZY < 4$. Hence such two regions support the propagating modes: $k = \theta_p/p$. In the first region, both Z and Y are negative that produce $\theta_p = -2\arcsin(\sqrt{ZY}/2)$, corresponding to the backward propagating mode; in the second region, both Z and Y are positive that produce $\theta_p = 2\arcsin(\sqrt{ZY}/2)$, corresponding to the forward propagating mode, as shown in Fig. 2.

In such two regions, the wave impedance $Z_0 = Z/[2\tan(\theta_p/2)]$ is always real and positive. Using the effective medium theory, the effective permittivity ϵ_{eff} and permeability μ_{eff} can be easily derived from the wavenumber and wave impedance, which have closed forms as

$$\mu_{\text{eff}} = L_{\text{eff}}\theta_p/\tan(\theta_p/2), \tag{13}$$

$$\epsilon_{\text{eff}} = C_{\text{eff}}\theta_p\tan(\theta_p/2), \tag{14}$$

where $L_{\text{eff}} = Z/(2\omega p)$ and $C_{\text{eff}} = 2/(Z\omega p)$ are effective inductance and capacitance, which can be either positive and negative. Apparently, the general circuit periodic structure is equivalent to a left-handed material in the frequency region $\omega_3 < \omega < \omega_1$ where both ϵ_{eff} and μ_{eff} are negative; and is equivalent to a right-handed material in the frequency region $\omega_2 < \omega < \omega_4$ where both ϵ_{eff} and μ_{eff} are positive.

In the region $\omega_1 < \omega < \omega_2$, we have $ZY < 0$. Hence it supports the pure plasma modes (see Fig. 2): $k = i\theta_I/p$, in which $\theta_I = 2\ln(\sqrt{-ZY/4} + \sqrt{-ZY/4+1})$. The corresponding wave impedance is a pure imaginary number in this case: $Z_0 = -iZ/[2\tanh(\theta_I/2)]$. Hence we can easily derive the effective permittivity ϵ_{eff} and permeability μ_{eff}

as

$$\mu_{\text{eff}} = L_{\text{eff}}\theta_I / \tanh(\theta_I/2), \tag{15}$$
$$\epsilon_{\text{eff}} = -C_{\text{eff}}\theta_I \tanh(\theta_I/2). \tag{16}$$

When $Z > 0$, we have $\mu_{\text{eff}} > 0$ and $\epsilon_{\text{eff}} < 0$, corresponding to an electric plasma; when $Z < 0$, we have $\mu_{\text{eff}} < 0$ and $\epsilon_{\text{eff}} > 0$, corresponding to a magnetic plasma.

In regions $0 < \omega < \omega_3$ and $\omega > \omega_4$, we have $ZY > 4$. Hence such two regions support the resonant crystal bandgap modes: $k = (\pi + i\theta_I)/p$, in which $\theta_I = 2\ln(\sqrt{ZY/4} + \sqrt{ZY/4 - 1})$. The wave impedance is also a pure imaginary number: $Z_0 = -iZ\tanh(\theta_I/2)/2$. Hence we easily obtain the effective permittivity ϵ_{eff} and permeability μ_{eff} as

$$\mu_{\text{eff}} = L_{\text{eff}}(\theta_I - i\pi)\tanh(\theta_I/2), \tag{17}$$
$$\epsilon_{\text{eff}} = C_{\text{eff}}(-\theta_I + i\pi)/\tanh(\theta_I/2). \tag{18}$$

Hence the general circuit periodic structure behaves like a crystal bandgap metamaterial in the frequency regions $0 < \omega < \omega_3$ and $\omega > \omega_4$. When $Z > 0$, then $\text{Re}\{\mu_{\text{eff}}\} > 0$ and $\text{Re}\{\epsilon_{\text{eff}}\} < 0$, and the metamaterial is electric-plasma type; when $Z < 0$, it is magnetic-plasma type.

From Eqs. (17) and (18), one of imaginary parts of the permittivity and permeability is always positive (indicating a positive loss), and the other is always negative (indicating a *negative loss*) [15]. They appear always in conjugate forms, which represents the lossless nature of the original circuit structure.

3. VALIDATION OF THE PROPOSED MEDIUM MODEL

We now choose arbitrarily the circuit parameters as $L_s = 20\,\text{nH}$, $L_p = 5\,\text{nH}$, $C_s = 2.5\,\text{pF}$, and $C_p = 2\,\text{pF}$. Then we get the four critical frequencies as $f_1 = 0.71\,\text{GHz}$, $f_2 = 1.59\,\text{GHz}$, $f_3 = 0.49\,\text{GHz}$, and $f_4 = 2.31\,\text{GHz}$. In such a condition, the wavenumber and wave impedance versus frequencies are illustrated in Fig. 3. From the dispersion curve shown in Fig. 3(a), we clearly observe that crystal bandgap mode is supported in the frequency band $f \in [0,\ 0.49)\,\text{GHz}$, backward propagating mode is supported in the frequency band $f \in [0.49,\ 0.71)\,\text{GHz}$, pure plasma mode is supported in the frequency band $f \in [0.71,\ 1.59)\,\text{GHz}$, forward propagating mode is supported in the frequency band $f \in [1.59,\ 2.31)\,\text{GHz}$, and crystal bandgap mode is supported again in the frequency band $f \in [2.31,\ \infty)\,\text{GHz}$, which are

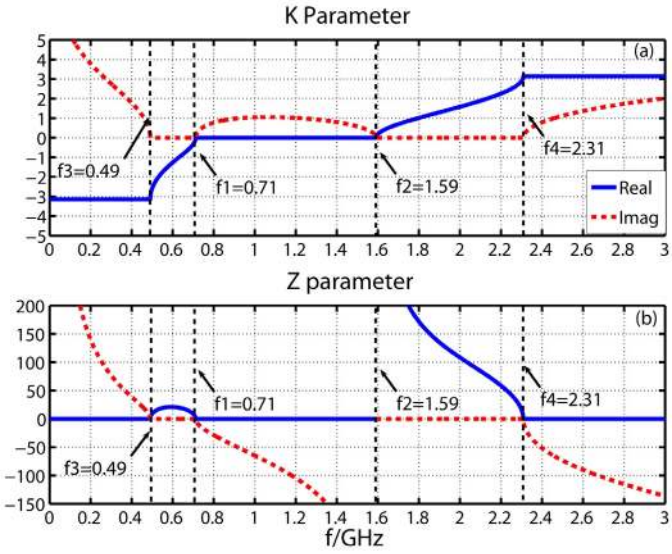

Figure 3. (a) The dispersion curve of the general periodic structure. (b) The wave impedance of the general periodic structure.

exactly the same as predicted earlier. Similar conclusion is drawn for the wave impedance.

Under the considered situation, the effective relative permittivity and permeability of the circuit structure are demonstrated in Figs. 4(a) and 4(b), respectively. From Fig. 4, we observe that the general structure is equivalent to a crystal bandgap metamaterial (magnetic-plasma type) in the frequency band $f \in [0,\ 0.49)$ GHz, a left-handed material in the frequency band $f \in [0.49,\ 0.71)$ GHz, a pure electric plasma in the frequency band $f \in [0.71,\ 1.59)$ GHz, a right-handed material in the frequency band $f \in [1.59,\ 2.31)$ GHz, and a crystal bandgap metamaterial (electric-plasma type) in the frequency band $f \in [2.31,\ \infty)$ GHz. They are also exactly coincident to earlier predictions.

From Fig. 4, we notice the conjugate imaginary parts of permittivity and permeability in the crystal bandgap regimes. In the frequency band $f \in [0,\ 0.49)$ GHz, the imaginary part of permittivity is positive, indicating a positive loss, while the imaginary part of permeability is negative, indicating a *negative loss*. The positive loss and negative loss cancel to each other to yield the lossless nature of the original periodic circuit. Similarly, in the frequency band $f \in [2.31,\ \infty)$ GHz, the effective permittivity has a negative loss, while

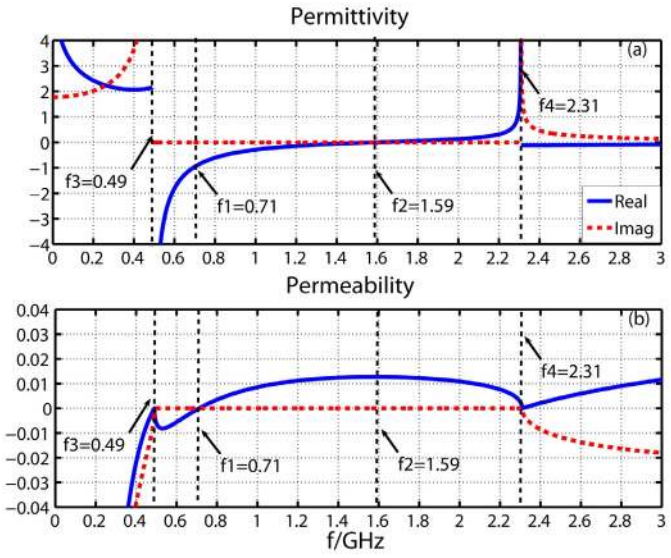

Figure 4. The effective medium parameters of the general periodic structure. (a) Permittivity. (b) Permeability.

the effective permeability has a positive loss. Such a phenomenon was never discovered in the earlier circuit medium models [1, 2].

In order to verify the correctness and accuracy of the equivalent medium models for different frequency regimes, we have computed the transmission coefficients (S_{21} parameters) of a ten-cell circuit structure in the whole frequency band, where the circuit parameters are given earlier. In the meantime, the ten-cell circuit structure can be equivalent to a medium slab, whose permittivity and permeability are given in Eqs. (13)–(18) in different frequency bands. Hence the transmission coefficient can also be calculated analytically for the effective medium slab using the electromagnetic wave theory [16].

To compare with the published equivalent medium model to periodic circuit structure, we rewrite the effective permittivity and permeability in [1, Eqs. (3.23a) and (3.23b)] as

$$\mu = \mu(\omega) = L_R^{'} - 1/(\omega^2 C_L^{'}), \tag{19}$$

$$\epsilon = \epsilon(\omega) = C_R^{'} - 1/(\omega^2 L_L^{'}). \tag{20}$$

The same formulations can be derived in [2, Eqs. (1.23) and (1.24)]. Hence we also calculate the transmission coefficient of the equivalent medium slab using Eqs. (19) and (20).

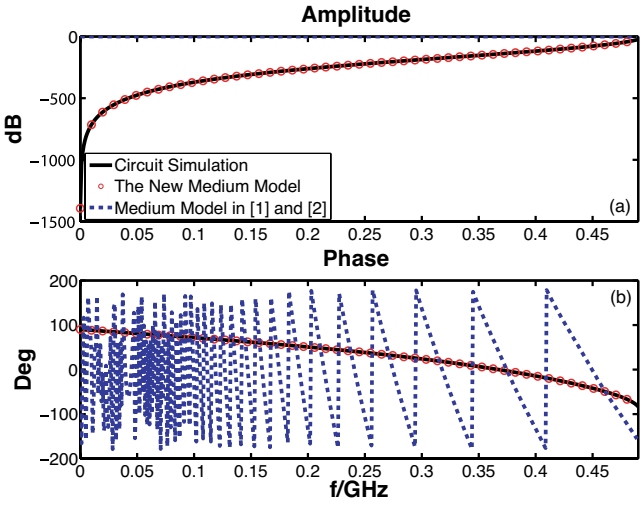

Figure 5. The transmission coefficients of a 10-cell periodic structure computed by circuit simulations and theoretical formulas of effective medium models in the frequency band $f \in [0,\ 0.49)$ GHz, the magnetic-plasma type crystal bandgap metamaterial region. (a) Amplitude. (b) Phase.

Figures 5–9 illustrate the comparison of computational results from circuit simulations and theoretical predictions from the new medium model and published medium model [1, 2] in different frequency regimes. Here, the circuit simulations are performed using the Agilent Advanced Design System (ADS). From these figures, we clearly observe that our theoretical predictions have excellent agreements with the circuit simulation results in the whole frequency band, implying the accuracy of the proposed medium models.

From Fig. 7, it is clear that the published effective medium parameters [1, 2], (19) and (20), are very accurate in the pure plasma region. But the new medium model is more accurate compared with the circuit simulation result. In the LH and RH material regions, however, the published formulas are accurate only in the frequency bands close to the pure plasma region, as shown in Figs. 6 and 8. In the crystal badgap metamaterial regions, the published effective medium parameters are invalid at all, as demonstrated in Figs. 5 and 9. The new medium model, however, is always very accurate in all frequency bands.

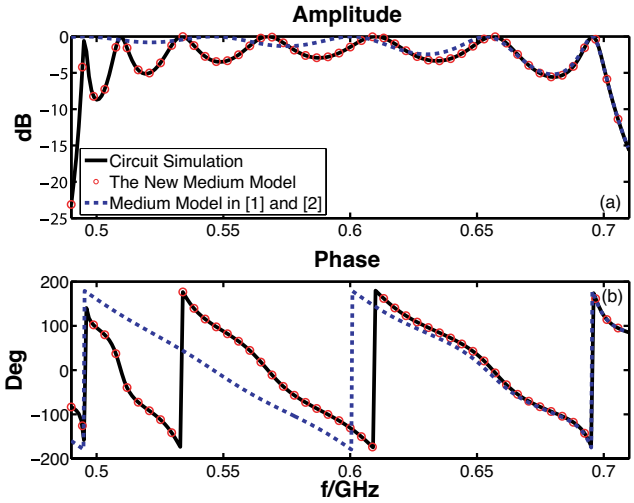

Figure 6. The transmission coefficients of a 10-cell periodic structure computed by circuit simulations and theoretical formulas of effective medium models in the frequency band $f \in [0.49,\ 0.71)$ GHz, the LH material region. (a) Amplitude. (b) Phase.

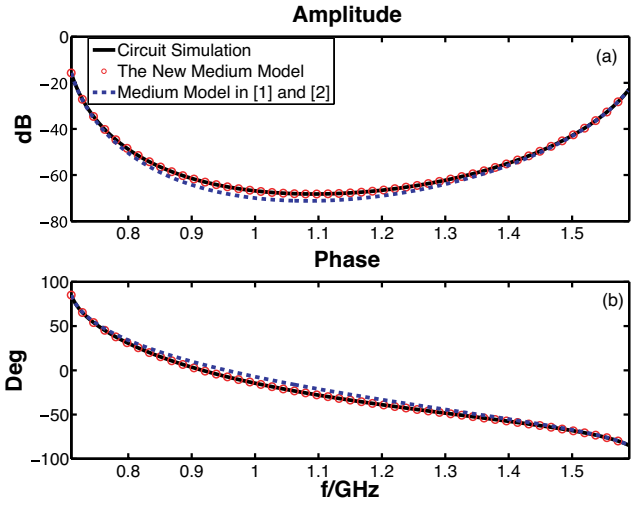

Figure 7. The transmission coefficients of a 10-cell periodic structure computed by circuit simulations and theoretical formulas of effective medium models in the frequency band $f \in [0.71,\ 1.59)$ GHz, the pure plasma region. (a) Amplitude. (b) Phase.

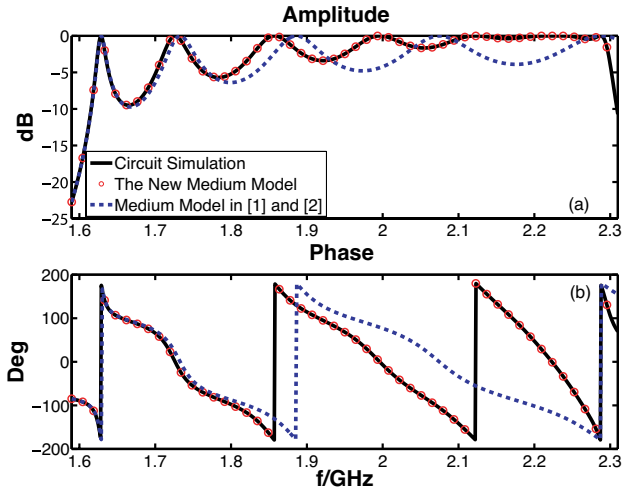

Figure 8. The transmission coefficients of a 10-cell periodic structure computed by circuit simulations and theoretical formulas of effective medium models in the frequency band $f \in [1.59,\ 2.31)$ GHz, the RH material region. (a) Amplitude. (b) Phase.

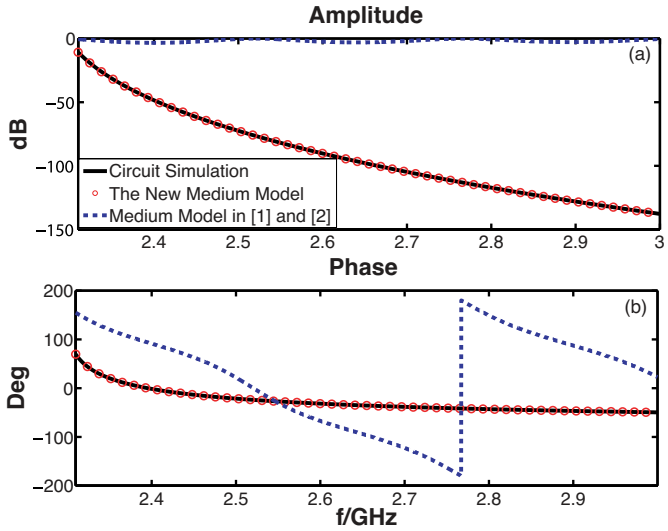

Figure 9. The transmission coefficients of a 10-cell periodic structure computed by circuit simulations and theoretical formulas of effective medium models in the frequency band $f \in [2.31,\ \infty)$ GHz, the electric-plasma type crystal badgap metamaterial region. (a) Amplitude. (b) Phase.

4. CONCLUSIONS

In conclusions, we can use a general symmetrical circuit periodic structure (see Fig. 1) to represent all kinds of metamaterials at different frequency bands. The effective medium models are given for all kinds of metamaterials with simple analytical formulations.

ACKNOWLEDGMENT

This work was supported in part by the National Basic Research Program (973) of China under Grant No. 2004CB719802, in part by the 111 Project under Grant No. 111-2-05, and in part by the National Science Foundation of China under Grant Nos. 60671015, 60496317, 60601002, and 60621002. Email: tjcui@seu.edu.cn.

REFERENCES

1. Caloz, C. and T. Itoh, *Electromagnetic Metamaterials: Transmission Line Theory and Microwave Applications*, 68, John Wiley & Sons, New York, 2004.
2. Eleftheriades, G. V. and K. G. Balmain, *Negative Refraction Metamaterials: Fundamental Properties and Applications*, 15, John Wiley & Sons, New York, 2005.
3. Mao, S. G. and Y. Z. Chueh, "Broadband composite right/left-handed coplanar waveguide power splitters with arbitrary phase responses and balun and antenna applications," *IEEE Transactions on Antennas and Propagation*, Vol. 54, 243–250, 2006.
4. Cui, T. J., Q. Cheng, Z. Z. Huang, and Y. J. Feng, "Electromagnetic wave localization using a left-handed transmission-line superlens," *Phys. Rev. B*, Vol. 72, 035112, 2005.
5. Alú, A. and N. Engheta, "Pairing an epsilon-negative slab with a mu-negative slab: resonance, tunneling and transparency," *IEEE Trans. Antennas Propagat.*, Vol. 51, 2558–2566, 2003.
6. Eleftheriades, G. V., "A generalized negative-refractive-index transmission-line (NRICTL) metamaterial for dual-band and quad-band applications," *IEEE Microwave Wireless Compon. Lett.*, Vol. 17, 415–417, 2007.
7. Eleftheriades, G. V., A. K. Iyer, and P. C. Kremer, "Planar negative refractive index media using periodically L-C loaded transmission lines," *IEEE Trans. Microwave Theory. Tech.*, Vol. 50, 2702–2710, 2002.

8. Lin, X. Q., Q. Cheng, R. Liu, D. Bao, and T. J. Cui, "Compact resonator filters and power dividers designed with simplified meta-structures," *Journal of Electromagnetic Waves and Applications*, Vol. 21, 1663–1672, 2007.
9. Li, Z. and T. J. Cui, "Novel waveguide directional couplers using left-handed materials," *Journal of Electromagnetic Waves and Applications*, Vol. 21, 1053–1062, 2007.
10. Guo, Y. and R. M. Xu, "Planar metamaterials supporting multiple left-hande dmodes," *Progress In Electromagnetics Research*, PIER 66, 239–251, 2006.
11. Wu, B.-I., W. Wang, J. Pacheco, X. Chen, T. M. Grzegorczyk, and J. A. Kong, "A study of using metamaterials as antenna substrate to enhance gain," *Progress In Electromagnetics Research*, PIER 51, 295–328, 2005.
12. Qin, Y. and T. J. Cui, "A general representation of left-handed materials using LC-loaded transmission lines," *Microwave Opt. Tech. Letts.*, Vol. 48, 2167–2171, 2006.
13. Liu, R., B. Zhao, X. Q. Lin, Q. Cheng, and T. J. Cui, "Evanescent-wave amplification studied using a bilayer periodic circuit structure and its effective medium model," *Phys. Rev. B*, Vol. 75, 125118, 2007.
14. Liu, R., T. J. Cui, B. Zhao, X. Q. Lin, H. F. Ma, D. Huang, and D. R. Smith, "Resonant crystal bandgap metamaterials in microwave regime and their exotic amplification of evanescent waves," *Appl. Phys. Lett.*, Vol. 90, 091912, 2007.
15. Liu, R., T. J. Cui, D. Huang, B. Zhao, and D. R. Smith, "Description and explanation of electromagnetic behaviors in artificial metamaterials based on effective medium theory," *Phys. Rev. E*, Vol. 76, 026606, 2007.
16. Kong, J. A., *Electromagnetic Wave Theory*, John Wiley & Sons, New York, 1986.
17. Yu, G. X. and T. J. Cui, "Imaging and localization properties of LHM superlens excited by 3D horizontal electric dipoles," *Journal of Electromagnetic Waves and Applications*, Vol. 21, 35–46, 2007.
18. Li, Z. and T. J. Cui, "Sandwich-structure waveguides for very-high power generation and transmission using left-handed materials," *Progress in Electromagnetics Research*, PIER 69, 101–116, 2007.
19. Li, Z., T. J. Cui, and J. F. Zhang, "TM wave coupling for high power generation and transmission in parallel-plate waveguide," *Journal of Electromagnetic Waves and Applications*, Vol. 21, 947–961, 2007.

20. Brovenko, A., P. N. Melezhik, A. Y. Poyedinchuk, and N. P. Yashina, "Surface resonances of metal stripe grating on the plane boundary of metamaterial," *Progress In Electromagnetics Research*, PIER 63, 209–222, 2006.
21. Chew, W. C., "Some reflections on double negative materials," *Progress In Electromagnetics Research*, PIER 51, 1–26, 2005.
22. Ishimaru, A., S. Jaruwatanadilok, and Y. Kuga, "Generalized surface plasmon resonance sensors using metamaterials and negative index materials," *Progress In Electromagnetics Research*, PIER 51, 139–152, 2005.
23. Yao, H.-Y., L.-W. Li, Q. Wu, and J. A. Kong, "Macroscopic performance analysis of metamaterials synthesized from micrsocopic 2-D isotropic cross split-ring resonator array," *Progress In Electromagnetics Research*, PIER 51, 197–217, 2005.